(28) Warner, M. *Mol. Cryst. Liq. Cryst.* **1982**, *80*, 79.
(29) Bawendi, M. G.; Freed, K. F. *J. Chem. Phys.* **1986**, *85*, 3007 and references therein.
(30) Gramsbergen, E. F.; Longa, L.; de Jeu, W. H. *Phys. Rep.* **1986**, *135*, 195.
(31) Flory, P. J. *Proc. Natl. Acad. Sci. U.S.A.* **1982**, *79*, 4510.
(32) Romanko, W. R. Master's Thesis, Northwestern University, 1987.
(33) Gujrati, P. D. *J. Phys. A: Math. Gen.* **1980**, *13*, 437.
(34) Gujrati, P. D.; Goldstein, M. *J. Chem. Phys.* **1981**, *74*, 2596.
(35) Baumgartner, A. *J. Chem. Phys.* **1986**, *84*, 1905.
(36) Flory, P. J. *Adv. Polym. Sci.* **1984**, *59*, 1.
(37) Ballauff, M.; Flory, P. J. *Ber. Bunsen-Ges. Phys. Chem.* **1984**, *88*, 530.
(38) Flory, P. J. *Principles of Polymer Chemistry*; Cornell University Press: Ithaca, NY, 1953.

Junction Fluctuations in Confined Chain Models of Rubber Elasticity

Douglas Adolf

Sandia National Laboratories, Albuquerque, New Mexico 87185.
Received November 14, 1987; Revised Manuscript Received February 5, 1988

ABSTRACT: The junction fluctuations in a micronetwork of entangled chains are examined and compared to the assumptions made by the constrained junction theories. The entanglements acting on the micronetwork chains are pictured as hoops of infinitesimal diameter through which a chain must pass. Over a limited range of the uniaxial extension ratio, the calculated fluctuations qualitatively agree with the constrained junction theories. Quantitative agreement is improved by allowing the hoops to have finite size. However, junction fluctuations are seen to have little effect on the uniaxial force of the micronetwork. The force is dominated by the strain dependence of the chain entropy. This implies that agreement in the junction fluctuations is not sufficient to infer that the constrained junction theories correctly model the primary effects of entanglements on network chains.

Introduction

All theories for the equilibrium elasticity of polymer networks rest on the assumption that the elastic force is primarily due to the change in entropy with strain of the covalently bonded network chains and that the noncovalent forces simply determine the isotropic pressure of the system.[1] To determine the force, then, one needs the probability distribution for the end-to-end vector for a network chain and the connectivity of the network itself. The simplest approach to rubber elasticity is to assume that the network is composed of Gaussian chains that are able to pass through each other freely and that the network junctions are fixed at their mean positions. This is the basis of the affine theory of rubber elasticity.[2] James and Guth[3] modified this approach to allow some of the network junctions to fluctuate in a self-consistent fashion (the phantom network theory). The force in response to uniaxial deformation for both of these theories is of the form $f \sim (\lambda - 1/\lambda^2)$, where λ is the uniaxial extension ratio. However, it is well-known that this strain dependence is incorrect for networks with chains of sufficient length.[1] The reduced force, $[f^*] = f/(\lambda - 1/\lambda^2)$, actually decreases with increasing extension ratio.

Modern theories attribute this strain dependence of the reduced force to entanglements that conserve network topology. Conserving topology exactly would result in an extremely difficult many-body problem, so the usual approach is to assume that each chain (or junction) is affected by entanglements in an average and independent fashion. The theories differ in how they model the effect of entanglements. One class of theories,[4,5] the constrained junction theories, assumes that the major effect of entanglements is to modify the network junction fluctuations. In the phantom network theory, the junction fluctuations are strain independent, whereas in the constrained junction theories, the fluctuations are assumed to be strain dependent. The chain statistics, however, are still assumed to be Gaussian, so the strain dependence of the reduced force is determined by the assumed strain dependence of the junction fluctuations. The other class of theories, the confined chain models, assume that the entanglements affect the entire chain. The effects of entanglements along the chain have been modeled as confining tubes,[6,7] slip-links,[8] and hoops through which the chain must pass.[9] In these theories, the fluctuations of the network junctions are neglected, so the strain dependence of the reduced force is dominated by the effect of the entanglements on the chain entropy.

In this paper, we are interested in the magnitude and strain dependence of the junction fluctuations for a finite-sized network composed of entangled chains using one type of confined chain model, the hoop model.[9] From this, we can determine if the assumed strain dependence of the junction fluctuations in the constrained junction theories is consistent with the predictions of this confined chain model. More importantly, we can see which effect of entanglements, that affecting chain entropy or junction fluctuations, dominates the reduced force.

Model and Theory

The hoop model envisions entanglements as hoops through which the polymer chain must pass. In general, these hoops may be of arbitrary size and placement. However, a simple analytical result is obtained only in the limit as the hoop diameter vanishes. We have previously shown,[9] that the partition function for such a chain with arbitrarily placed hoops is given by

$$Q = \frac{\sum_1^M t_i}{\prod_1^M t_i} \exp\left(-\frac{3}{2Nl^2}\sum_1^M t_i^2\right) \qquad (1)$$

where N is the number of segments each of length l on a

0024-9297/88/2221-2249$01.50/0

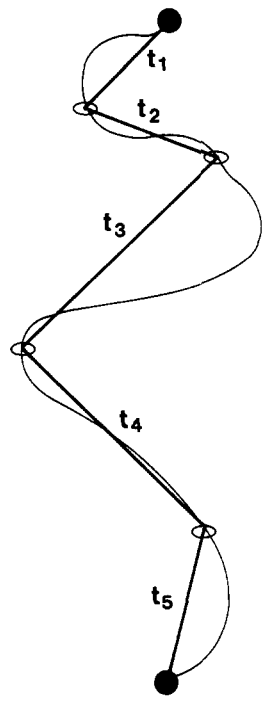

Figure 1. Entangled network chain as pictured by the hoop model; here, $M = 5$.

network chain, $M - 1$ is the number of hoops, and t_i is the distance between hoops (see Figure 1). If we assume that the hoops are equally spaced (i.e., $t_i = t$ for all i), eq 1 becomes

$$Q \sim \frac{\exp\left(-\frac{3L^2}{2Nl^2}\right)}{L^{M-1}} \tag{2}$$

where $L = \sum t_i = Mt$ can be related to the "primitive path" concept of reptation theory.[10] Equation 2 now represents an unnormalized probability distribution for the primitive path contour length, L.

It is clear that this distribution becomes infinite at $L = 0$, which is unphysical. The reason for this behavior is given in Appendix A, where an exact calculation for the case $M = 2$ is given. Equation 2 is shown to be valid for $L > L^*$ with $L^*/N^{1/2}l \ll 1$. Below L^*, Q levels off. In the subsequent calculations, Q will be approximated by using eq 2 for $L > L^*$ and $Q(L) = Q(L^*)$ for $L < L^*$.

We now calculate the junction fluctuations for a network composed of these chains. To do this for an infinite network is difficult. A more reasonable approach is to work with the rank-one micronetwork shown in Figure 2. Here, three chains are attached at a junction that is allowed to fluctuate, and the remaining three chain ends are fixed in space. Uniaxial extension is simulated by moving these fixed chain ends affinely with strain. The mean-square junction fluctuation is found by using the equation

$$\langle \delta y_i^2 \rangle = \langle y_i^2 \rangle - \langle y_i \rangle^2 = Z^{-1} \int_V \mathrm{d}\mathbf{r}\; y_i^2 P(R_1)\, P(R_2)\, P(R_3) \tag{3}$$

where $\mathbf{r} = (y_1, y_2, y_3)$ is the position of the junction, $\langle y_i \rangle = 0$ by construction, Z is the normalizing partition function for the micronetwork given by

$$Z = \int_V \mathrm{d}\mathbf{r}\; P(R_1)\, P(R_2)\, P(R_3) \tag{4}$$

and $P(R_i)$ gives the distribution for the end-to-end distance of chain i.

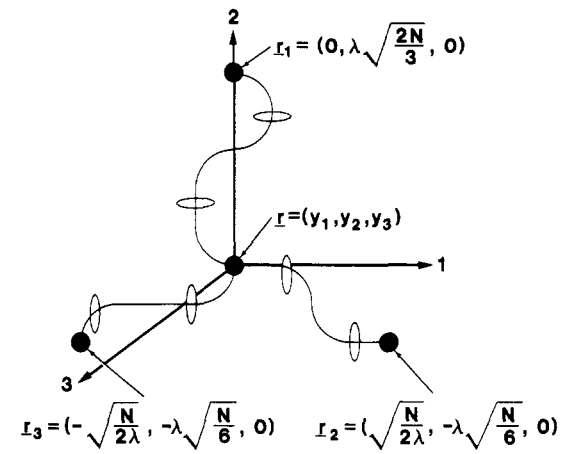

Figure 2. Entangled rank-one micronetwork with the chains. The fixed chain ends deform affinely with the uniaxial strain while the junction r is free to fluctuate.

As yet, we do not have an expression for $P(R)$. Equation 2 represents the statistical weight for a given primitive path, which, in principle, is related to $P(R)$ by

$$P(R) \sim \int_0^\infty \mathrm{d}L\; Q(L)\, P(R|L) \tag{5}$$

where $P(R|L)$ is the conditional probability for the end-to-end distance with a given primitive path. The simplest approach is to assume that the conditional probability for the end-to-end distance, $P(R|L)$, is sharply peaked about its mean such that

$$P(R|L) \sim \delta(R^2 - \langle R^2(L) \rangle) \sim \delta(R^2 - L^2/M) \tag{6}$$

where $\langle R^2 \rangle$ (or equivalently L^2) is dependent on the extension ratio. Equation 6 is exact for a micronetwork that allows no junction fluctuations and is a good approximation for micronetworks in which the junction fluctuations are small compared to the mean end-to-end distance of the network chains. It is shown later that this corresponds to highly entangled networks. From eq 5 and 6, $P(R)$ is given by

$$P(R) \sim \frac{\exp\left(-\frac{3MR^2}{2Nl^2}\right)}{R^{M-1}} \tag{7}$$

where L^2 has been replaced by MR^2. Again, eq 7 becomes infinite as R approaches 0. However, as before, we will approximate $P(R)$ by using eq 7 for $R > R^*$ and letting $P(R) = P(R^*)$ for $R < R^*$, where $R^* = L^*/M^{1/2}$.

Equation 7 also exhibits the phenomenon of "network collapse"; that is, $\langle R^2 \rangle$ for an isolated chain calculated from eq 7 is independent of N. This is a familiar problem that occurs whenever constraints are placed on Gaussian chains. For example, the dimension of a Gaussian chain collapses when it is cross-linked internally,[11] and the overall dimension of a network composed of end-linked Gaussian chains collapses.[12,13] The standard procedure to avoid network collapse is to fix some cross-links in space at physically realistic positions.[2] The same procedure is employed here in that the three stationary chain ends of the rank-one micronetwork are placed such that $\langle R^2 \rangle \sim N$ for each chain. The exact placement of the fixed ends follows the discussion in ref 14.

The micronetwork junction fluctuations can now be expressed as

$$\langle \delta y_i^2 \rangle = Z^{-1} \int_V \mathrm{d}\mathbf{r}\; [y_i^2 \exp\{-\beta^2 \sum_1^3 (\mathbf{r}_j - \mathbf{r})^2\}] e^{-(M-1)h(r)} \tag{8}$$

where $\beta^2 = 3/2Nl^2$, $\mathbf{r}_j$ is the strain-dependent position of the fixed end for chain j, and $h(r)$ is given by

$$h(r) = \beta^2 \sum_1^3 (\mathbf{r}_j - \mathbf{r})^2 + \tfrac{1}{2} \sum_1^3 \ln (\mathbf{r}_j - \mathbf{r})^2 \qquad (9)$$

For large values of M, eq 8 can be solved by the method of steepest descents. The details are given in Appendix B. The junction fluctuations parallel and perpendicular to the uniaxial strain are found to be

$$\langle \delta y^2 \rangle_\parallel = \frac{\langle \delta y^2 \rangle_{PN}/M}{1 - s(\lambda)} \qquad \langle \delta y^2 \rangle_\perp = \frac{\langle \delta y^2 \rangle_{PN}/M}{1 + s(\lambda)} \qquad (10)$$

where $\langle \delta y^2 \rangle_{PN}$ is the mean-square junction fluctuation in the unentangled phantom network (equal to $Nl^2/9$ in this micronetwork) and $s(\lambda)$ is

$$s(\lambda) = \frac{2}{9} \frac{\frac{1}{2\lambda} - \frac{1}{6}(\lambda - 2k)^2}{\left[\frac{1}{2\lambda} + \frac{1}{6}(\lambda - 2k)^2\right]^2} - \frac{1}{6(\lambda + k)^2} \qquad (11)$$

In the above, k is also a function of the uniaxial extension ratio, λ, and is shown to be

$$k(\lambda) = \frac{4\lambda^4 - \lambda^2 - 3}{6\lambda^4 + 8\lambda^3 + 19\lambda^2 + 3} \qquad (12)$$

The force in response to a uniaxial deformation in the limit of large M can also be obtained by the method of steepest descents. As shown in Appendix B, the micronetwork force is approximately

$$f = f_F - \frac{\partial V_f/\partial \lambda}{V_f} \qquad (13)$$

where f_F is the force for the corresponding entangled micronetwork in which the junction is not free to fluctuate but is fixed at its mean position. V_f is the "fluctuation volume" equal to $(\langle \delta y_1^2 \rangle \langle \delta y_2^2 \rangle \langle \delta y_3^2 \rangle)^{1/2}$.

For less entangled chains (i.e., smaller M), the junction fluctuations must be found by numerically integrating eq 3 with $P(R)$ given by eq 7 with use of the appropriate cutoff, R^*. The uniaxial force is found by numerical integration of the partition function, eq 4, and by use of the formula $f = -\partial \ln Z/\partial \lambda$.

Results and Discussion

From eq 10, we see that the mean-square junction fluctuations in the unstrained state for large M are predicted to vary as Nl^2/M. Again, M is the number of "subchains" spanning the $M - 1$ hoops, and it is reasonable to assume that M is proportional to N/N_e, where N_e is the entanglement degree of polymerization. This implies that the fluctuations in the unstrained state are proportional to $N_e l^2$ and are independent of the molecular weight of the network chains. This relationship is also observed in the numerical results for chains with smaller values of M (M = 2 and 4). Therefore, the mean-square junction fluctuations for all M are of the form

$$\langle \delta y_i^2 \rangle = \frac{N_e l^2}{9} g_i(\lambda, M) \qquad (14)$$

where the subscript i refers to the axis of interest and $g_i(1,M) = 1$.

Figures 3 and 4 plot the functions g_2 and g_1 (parallel and perpendicular to the uniaxial extension) respectively for $1 < \lambda < 3$. Experimentally, one cannot usually extend a sample beyond about $\lambda = 3$ or 4 due to crystallization or rupture. Roughly speaking, the calculated junction fluctuations parallel to the uniaxial extension increase with increasing extension ratio and those perpendicular decrease. This is in qualitative agreement with the assumptions of the constrained junction theories. However, there are significant differences. For instance, the parallel fluctuations do not eventually plateau at the phantom network value, $\langle \delta y^2 \rangle = Nl^2/9$. They are consistently lower. It appears as if the parallel fluctuations plateau at some lower value. In fact, the micronetwork fluctuations along all axes slowly approach the unstrained value as the extension ratio is increased. Additionally, the observed strain dependence of the junction fluctuations is less than that assumed by the constrained junction theories.

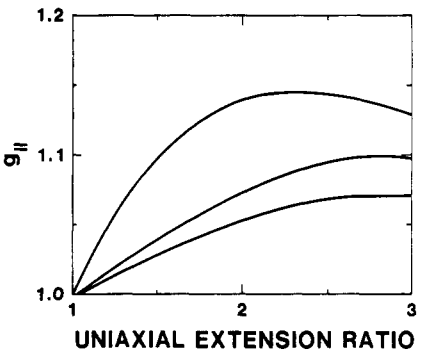

Figure 3. Normalized mean-square junction fluctuations parallel to the uniaxial extension versus λ.

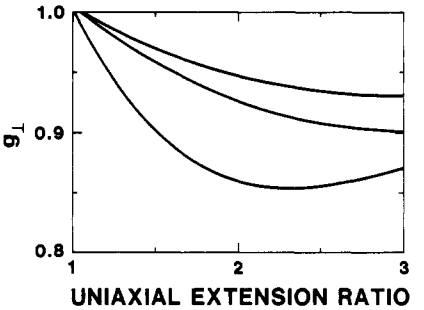

Figure 4. Normalized mean-square junction fluctuations perpendicular to the uniaxial extension versus λ.

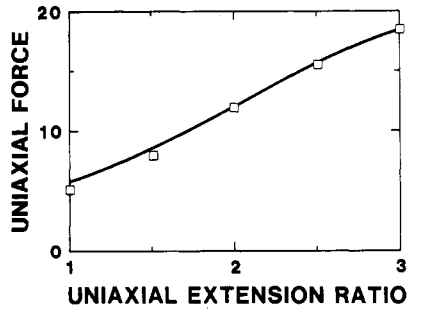

Figure 5. Uniaxial force for the micronetwork with (symbols) and without (line) junction fluctuations versus λ. Junction fluctuations have little effect on the uniaxial force.

Experimentally, a more important question is what is the importance of junction fluctuations on the uniaxial force. For an answer to this question, the micronetwork uniaxial force was compared to the force calculated for the analogous micronetwork for which the junction was fixed at its mean position and not allowed to fluctuate. The two results are shown in Figure 5 for chains with M = 2, which should show the most difference. As can be seen, there is no noticeable difference, implying that the strain dependence of the chain entropy overwhelms the contribution of the junction fluctuations. This is also seen in eq 13, giving the uniaxial force for large M. Two points should be made. First, the "fluctuation volume" varies little as the extension ratio is increased, so the contribution of the

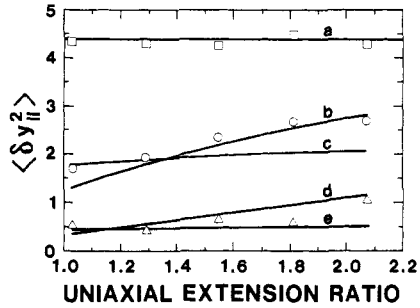

Figure 6. Mean-square junction fluctuations parellel to the uniaxial extension versus λ: simulation results[14] for N_e = infinity (□), 16 (○), and 4 (△) and chains with 40 segments; line a, phantom micronetwork result; lines b and d, best fits to the Flory constrained junction theory; lines c and e, hoop model predictions with N_e = 16 and 4 respectively (no adjustable parameters).

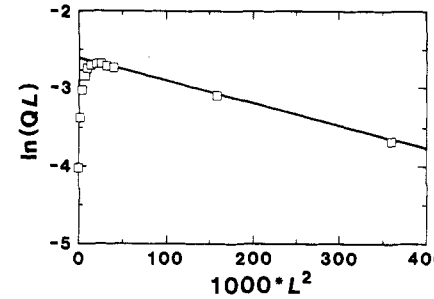

Figure 7. Primitive path distribution Q (symbols) calculated from eq 17 and plotted as ln $Q(L)$ versus L^2, where $L = L/N^{1/2}l$ is the reduced primitive path length. The line shows the relation $Q \sim [\exp(-3L^2/2)]/L$ (eq 2 for M = 2). The deviation of the symbols from the line is due to Q leveling off at small L (i.e., Q does not diverge as L approaches 0).

second term in eq 13 is small. Second, the first term in eq 13 is proportional to M, whereas the second term is not (this is shown in Appendix B). Therefore, as M becomes large, the contribution of the junction fluctuations to the uniaxial force becomes negligible and the practice of ignoring junction fluctuations in determining the force becomes exact.

As stated earlier, the hoop model was solved analytically for hoops of infinitesimal diameter. If the hoops are allowed to have finite size, which itself is strain dependent, one might expect that the junction fluctuations become more strongly strain dependent. We previously examined a closely related model by computer simulation.[14] The results for the fluctuations parallel to the uniaxial extension are shown in Figure 6 for N_e of infinity (unentangled), 16, and 4 over the limited extension ratio range of $1 \leq \lambda \leq 2.25$. The hoop model and best fit constrained junction fluctuations are included for comparison. The junction fluctuations calculated from the simulation were found to follow eq 14 as in the hoop model. However, allowing for finite-sized hoops does increase the strain dependence of the fluctuations (i.e., of the function $g_i(\lambda,M)$) and improves agreement with the constrained junction theories. It is not clear that the computer simulation fluctuations plateau at the phantom network ($N_e = \infty$) value or that the fluctuations play a significant role in determining the level of the uniaxial force as assumed in the constrained junction theories. Further studies are planned to address the latter point.

It is also of interest to see the predictions of another type of confined chain model for the micronetwork junction fluctuations. For instance, the tube models predict that the primitive path distribution is of the form

$$P(L) = K(\lambda) \exp\left(-\frac{3L^2}{2Nl^2}\right) \qquad (15)$$

where $K(\lambda)$ is strain dependent due to the strain dependence of the tube diameter. If $P(L)$ is related to $P(R)$ as above by simply replacing L with MR, it can be shown easily that the junction fluctuations are smaller than in the corresponding phantom network by a factor of M but are still strain independent.

Conclusions

The junction fluctuations for one type of confined chain model, the hoop model, have been shown to agree qualitatively with the assumptions of the constrained junction theories over an experimentally accessible range of uniaxial extension ratios. However, a quantitative agreement is lacking. Apparent agreement can be improved by allowing the hoops to have finite and strain-dependent size. One must be careful in interpreting that the agreement in junction fluctuations indicates that the force derived from the two theories agree also. The hoop model uniaxial force, calculated by using infinitesimal diameter hoops and allowing junction fluctuations, is dominated by the strain dependence of the chain entropy, which is in sharp contrast to the predictions of the constrained junction theories. Therefore, if one could experimentally determine the junction fluctuations of a polymer network and observe the behavior predicted by constrained junction theories, it still does not offer conclusive evidence that these theories capture the true physics.

Acknowledgment. This work was performed at Sandia National Laboratories supported by the U.S. Department of Energy under Contract No. DE-AC04-76DP00789.

Appendix A: Apparent Divergence of $Q(L)$ at $L = 0$

As stated previously, the primitive path distribution given in eq 2 diverges as L approaches 0. The reason for this is clear when one examines the origin of the partition function for, say, M = 2. In this case, the partition function is obtained from

$$Q = \int_0^N dn \left[\frac{3}{2\pi n l^2}\right]^{3/2} \exp\left[-\frac{3t_1^2}{2nl^2}\right] \times \left[\frac{3}{2\pi(N-n)l^2}\right]^{3/2} \exp\left[-\frac{3t_2^2}{2(N-n)l^2}\right] \qquad (16)$$

where t_i is the distance between the ith end of the chain and the hoop. When t_i and n or $N - n$ are both equal to zero, the integrand becomes indefinite. That the integral may diverge is simply an artifact of the Gaussian distribution used in the continuous representation of the chain and dependent on the order in which the limits $t \to 0-$ and $n \to 0$ are taken. In ref 9, the partition function for arbitrary M was calculated by Laplace transformation of the convolution product in the segment variable and subsequent inversion. This allows analytical solution of the problem but effectively takes the limits in the incorrect order, resulting in the divergence of $Q(L)$ as $L \to 0$.

An exact formulation of the partition function for the case of equal subchain length ($t_1 = t_2$) and a discrete chain is given by

$$Q\left(\frac{L}{N^{1/2}l}\right) = Q(L) \sim \sum_1^N \frac{1}{[i(1-i/N)]^{3/2}} \exp\left[-\frac{3L^2}{8(i/N)(1-i/N)}\right] \qquad (17)$$

for $L > 0$. As seen in Figure 7, eq 17 is equivalent to $Q(L) \sim [\exp(-3L^2/2)]/L$, which is eq 2 with $M = 2$, for $L > 0.1$ and levels off for values less than 0.1. Therefore, the partition function is approximated well by using eq 2 for $L > L^*$ and $Q(L) = Q(L^*)$ for $L < L^*$. The results for the junction fluctuations and force are fairly insensitive to the exact value of L^* chosen.

Appendix B: Results for Large M by the Method of Steepest Descents

The mean-square junction fluctuations and the uniaxial force for the micronetwork both can be expressed in terms of the integral

$$l_\alpha^{\,i} = \int_V \mathrm{d}\mathbf{r}\; w_a^{\,i}(r)\; e^{-Mh(r)} \tag{18}$$

where $w_\alpha^{\,i}(r)$ is given by

$$w_\alpha^{\,i}(r) = y_i^{\alpha} \exp[-\beta^2 \sum_1^3 (\mathbf{r}_j - \mathbf{r})^2] \tag{19}$$

From the above, $\langle \delta y_i^2 \rangle = l_2^{\,i}/l_0$ and $f = -\partial \ln l_0/\partial\lambda$.

The integral l_α can be solved by the method of steepest descents for large M.[15] The first step is to find the position of the junction for which $\partial h/\partial y_i$ vanishes. The resulting position is $r^* = (0,-N^{1/2}lk,0)$, where $k(\lambda)$ is given by eq 12. The second step is to calculate the second derivatives of h, $h_{ij} = \partial^2 h/\partial y_i \partial y_j$, evaluated at r^*. The cross terms ($i \neq j$) vanish, and $(Nl^2/9)h_{11} = 1 + s(\lambda)$ and $(Nl^2/9)h_{22} = 1 - s(\lambda)$, where s is given by eq 11. The integrals l_α can then be expressed as

$$l_\alpha^{\,i} = e^{-\beta^2 Mh(r^*)} \int_{-\infty}^{\infty} \mathrm{d}y_i\; y_i^{\alpha} \exp[-\beta^2(3 + \tfrac{1}{2}Mh_{ii})y_i^2] \prod_{j \neq i} \int_{-\infty}^{\infty} \mathrm{d}y_j \exp[-\beta^2(3 + \tfrac{1}{2}Mh_{jj})y_j^2] \tag{20}$$

Evaluating the integrals results in eq 10 for the junction fluctuations and the following for the partition function:

$$-\ln Z \sim \beta^2 Mh(r^*) + \tfrac{1}{2}\sum_1^3 \ln h_{ij} \tag{21}$$

where only the strain-dependent portion of the partition function has been retained.

The uniaxial force is found by differentiating eq 21 with respect to the extension ratio, which results in

$$f = f_F + \frac{1}{2}\sum_1^3 \frac{\partial h_{ii}/\partial\lambda}{h_{ii}} = f_F - \frac{1}{2}\sum_1^3 \frac{\partial \langle \delta y_i^2 \rangle/\partial\lambda}{\langle \delta y_i^2 \rangle} \tag{22}$$

where f_F is the free energy of the network with the junction fixed at its most probable position (from the first term in eq 21). With the "fluctuation volume" defined as $(\langle \delta y_1^2 \rangle \langle \delta y_2^2 \rangle \langle \delta y_3^2 \rangle)^{1/2} \cong \langle \delta y^2 \rangle^{3/2}$ due to the relatively weak strain dependence of the junction fluctuations, the force can be approximately represented by eq 13.

References and Notes

(1) Treloar, L. R. G. *The Physics of Rubber Elasticity*; Oxford University Press: London, 1958.
(2) Flory, P. J. *Principles of Polymer Chemistry*; Cornell University Press: Ithaca, NY, 1956.
(3) James, H. M.; Guth, E. *J. Chem. Phys.* **1943**, *11*, 455.
(4) Ronca, G.; Allegra, G. *J. Chem. Phys.* **1975**, *63*, 4990.
(5) Flory, P. J. *J. Chem. Phys.* **1977**, *66*, 5720.
(6) Marrucci, G. *Macromolecules* **1981**, *14*, 434.
(7) Gaylord, R. J. *Polym. Bull.* **1983**, *9*, 156.
(8) Ball, R. C.; Doi, M.; Edwards, S. F.; Warner, M. *Polymer* **1981**, *22*, 1010.
(9) Adolf, D. *Macromolecules* **1987**, *20*, 116.
(10) Doi, M.; Edwards, S. F. *The Theory of Polymer Dynamics*; Oxford University Press: Oxford, 1986.
(11) Allen, G.; Burgess, J.; Edwards, S. F.; Walsh, D. J. *Proc. R. Soc., London* **1973**, *A334*, 453.
(12) Ronca, G.; Allegra, G. *J. Chem. Phys.* **1975**, *63*, 4104.
(13) Martin, J. E.; Eichinger, B. E. *Macromolecules* **1980**, *13*, 626.
(14) Adolf, D.; Curro, J. G. *Macromolecules* **1987**, *20*, 1646.
(15) Wyld, H. W. *Mathematical Methods for Physics*; Addison-Wesley: Reading, MA, 1979.

Investigation of Relaxation Processes in Low and High Molecular Weight Bulk Poly(methyl methacrylate) by Dynamic Light Scattering

G. Fytas*

Research Center of Crete and Department of Chemistry, University of Crete, Iraklion, Crete, Greece

C. H. Wang

Department of Chemistry, University of Utah, Salt Lake City, Utah 84112

E. W. Fischer

Max Planck Institut fur Polymerforschung, P.O. Box 3148, 6500 Mainz, FRG.

Received July 27, 1987; Revised Manuscript Received January 13, 1988

ABSTRACT: Photon correlation functions of the polarized component of the scattered light from a low molecular weight PMMA (M_w = 3900, T_g = 52 °C) have been studied in the temperature range 65–98 °C. The observed relaxation functions have been represented by a multiexponential decay by using an inverse Laplace transform analysis. The computed spectrum of retardation times reveals a two-peak structure like that observed in the high molecular weight material (T_g = 107 °C). The temperature dependences of the long-time peak associated with the primary glass–rubber relaxation in the two PMMA's are similar when compared at temperatures equidistant from their T_g's. The light scattering and ultrasonic data on the longitudinal density fluctuations over 12 decades in time conform to a single Vogel–Fulcher–Tamman–Hesse equation. The relaxation times of the short-time peak in the retardation spectrum are insensitive to T_g and compare favorably with dielectric data associated with the secondary β-relaxation.

Introduction

Dynamic light scattering has proved to be a potential method for the study of bulk polymer dynamics near and above the glass transition temperature (T_g). The dynamics of the thermodynamic fluctuations in the density and optical anisotropy in the time range 10^{-6}–10^2 s can be

0024-9297/88/2221-2253$01.50/0